J. Math. Biol. 41, 455–475 (2000)
Digital Object Identifier (DOI):
10.1007/s002850000038

Mathematical Biology

Rebecca Tyson · L.G. Stern · Randall J. LeVeque

Fractional step methods applied to a chemotaxis model

Received: 18 October 1998 / Published online: 23 October 2000 – © Springer-Verlag 2000

Abstract. A fractional step numerical method is developed for the nonlinear partial differential equations arising in chemotaxis models, which include density-dependent diffusion terms for chemotaxis, as well as reaction and Fickian diffusion terms. We take the novel approach of viewing the chemotaxis term as an advection term which is possible in the context of fractional steps. This method is applied to pattern formation problems in bacterial growth and shown to give good results. High-resolution methods capable of capturing steep gradients (from CLAWPACK) are used for the advection step, while the A-stable and L-stable TR-BDF2 method is used for the diffusion step. A numerical instability that is seen with other diffusion methods is analyzed and eliminated.

1. Introduction

Many organisms exhibit a biased random walk in the presence of a chemical. This motion is termed chemotaxis, and often results in very interesting spatial patterns. Mathematical models of the biological system are an important tool used in the investigation of these patterns. Chemotaxis systems are highly nonlinear, due to the negative density-dependent diffusion term which characterises chemotactic behaviour, and so any realistic model is too difficult to solve analytically. Thus numerical simulation is a crucial part of the analysis.

These models are time-dependent systems of partial differential equations, typically in two or three space dimensions, which contain three distinct sets of terms modeling three distinct processes:

- Reaction terms, modeling the interaction of different components, *e.g.*, consumption of nutrients, growth of cells, release of chemoattractant, etc.,

R. Tyson: Department of Applied Mathematics, Box 352420, University of Washington, Seattle, WA 98195-2420, USA. e-mail: rebecca@amath.washington.edu

L.G. Stern: Cray Inc., 411 First Avenue South, Suite 600, Seattle, WA 98104-2860, USA. e-mail: stern@cray.com

R.J. LeVeque: Departments of Mathematics and Applied Mathematics, University of Washington, Seattle, WA 98195, USA. e-mail: rjl@amath.washington.edu

Key words: Chemotaxis – Bacterial growth – Pattern formation – Numerical – Fractional step – CLAWPACK

- Diffusion terms, modeling the random motion of each component,
- Chemotaxis terms, which we will view as advection terms, modeling the directed motion of one or more component in response to concentration gradients of another component (the chemoattractant).

Reaction-diffusion equations including only the first two processes above have been widely studied, both theoretically and numerically, as models of many biological systems. Chemotaxis adds the new ingredient of negative density-dependent diffusion, and the development of numerical methods for this problem has not been studied as intensively to date.

In this paper we discuss the appropriate ingredients of a *fractional step method* for such problems, in which the three processes are decoupled and numerical methods best suited for each step are applied sequentially. This has several advantages over an "unsplit" method in which all terms are modeled simultaneously, as outlined in subsequent sections. It also allows us to view the chemotaxis term as an advection term, which can be treated very accurately when separated from diffusive processes. Here we study one particular model for pattern formation in bacteria, but similar methods should be useful for many other problems in chemotaxis.

In particular, we focus on the following issues:

1. The use of high-resolution slope-limiter methods for the advection step, as implemented in the CLAWPACK software package, which is freely available[9]. This class of methods was originally developed for accurately computing shock waves and other discontinuous solutions in compressible gas dynamics, and gives sharp resolution of rapidly varying solutions without nonphysical oscillations. These methods are ideal for pattern formation problems where sharp peaks in concentration arise in localized areas. To our knowledge these methods have not been previously applied in chemotaxis problems.
2. The second-order accurate, L-stable TR-BDF2 method for the reaction and diffusion steps. This method is not nearly as well known as standard second-order methods such as Crank-Nicolson, but its use is critical for this problem.
3. Using the Crank-Nicolson method for the diffusion step can lead to a subtle numerical instability due to a nonlinear interaction between the advection and reaction steps. We explain this instability and demonstrate that use of the TR-BDF2 method restores stability and results in an efficient and accurate solution procedure for the full chemotaxis model.

While each component of our solution procedure is a standard numerical approach in other fields, this particular combination of methods coupled through fractional steps gives a new and powerful method for chemotaxis problems which should be applicable more generally. Each component will be discussed in detail starting in Section 4. First we introduce the particular chemotaxis model used as an example in this paper.

2. Bacterial patterns and a mathematical model

Recently, Budrene and Berg (1991, 1995) have shown that a colony of *E. coli* or *S. typhimurium* will form geometrically complex patterns when exposed to, or

feeding on, intermediates of the tricarboxylic acid (TCA) cycle, particularly succinate. In response to succinate, the bacteria secrete aspartate which is a potent chemoattractant. The bacteria, aspartate and succinate are the critical players in the experiments.

The patterns formed by *S. typhimurium* are concentric rings which are either continuous or spotted [26]. Initially succinate is uniformly distributed throughout a thin layer of medium, and an inoculum of cells is added to the centre. The patterns begin with the formation of a very low density bacterial lawn spreading out discwise from the initial inoculum. Stationary, high density rings of bacteria appear within this lawn.

E. coli forms complex patterns including sunflower spirals, radial spots, radial stripes and chevrons [5]. The initial conditions are the same as for the *S. typhimurium* experiments, but the pattern mechanism is quite different. Initially, instead of a thin bacterial lawn, a swarm ring (high density ring of vigorously motile bacteria) forms and expands outwards from the initial inoculum. The bacterial density in the swarm ring increases until some point at which the ring becomes unstable, and some percentage of the bacteria are left behind as aggregates. These aggregates remain bright (full of vigorously motile bacteria) for a short period of time, but then dissolve as the bacteria rejoin the swarm ring. Left behind in the aggregate's original location is a clump of bacteria which, for some as yet unknown reason (biologically), are non motile. These non-motile bacteria remain as markers of the pattern.

For all of these patterns the essential building blocks of bacteria, aspartate (chemoattractant) and succinate (pattern stimulant) remain the same. The important biological processes in these experiments are diffusion of bacteria, aspartate and succinate, proliferation of bacteria, secretion and uptake of aspartate by the bacteria, consumption of succinate, and chemotaxis of the cells up gradients of aspartate. The cells both secrete and consume the aspartate. Also, proliferation includes reproduction and death of the cells. Though the cells do not actually die, they are known to become non-motile and cease participating in the formation of pattern. Thus, for the purposes of the model these cells are considered dead.

Combining the key biological processes into a mathematical model, we arrive at a system of three partial differential equations of the form

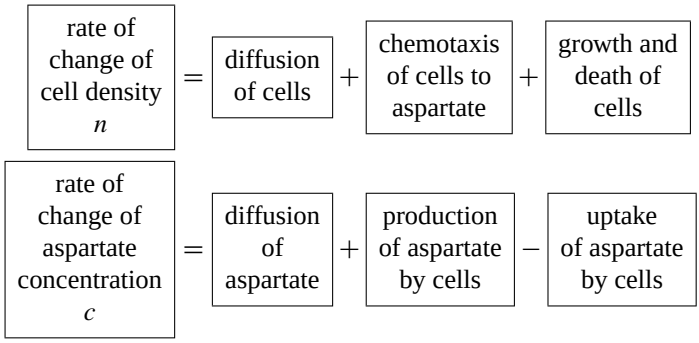

$$\boxed{\begin{array}{c}\text{rate of}\\ \text{change of}\\ \text{succinate}\\ \text{concentration}\\ s\end{array}} = \boxed{\begin{array}{c}\text{diffusion}\\ \text{of}\\ \text{succinate}\end{array}} - \boxed{\begin{array}{c}\text{uptake}\\ \text{of succinate}\\ \text{by cells}\end{array}} \tag{1}$$

where n denotes bacterial cell density, c aspartate concentration and s succinate concentration. All quantities are nondimensional. The presence of diffusion terms and chemotaxis terms is basic to chemotaxis models. It is fundamentally the interaction of Fickian diffusion, which tends to erase pattern, and chemotaxis, which tends to enhance it, which creates the stable spatial patterns observed. The two processes are equally important, and the nonlinear nature of the chemotaxis term is crucial. The general form of this term is $\nabla(u\chi(v))$ where u represents cell density and v represents chemoattractant density. The generally nonlinear function $\chi(v)$ is the cellular diffusion rate up the chemoattractant density gradient, which varies with the local chemoattractant concentration.

For many of the boxed terms, functional forms substantiated by experimental results are available in the literature. Using these and expressions motivated by the particulars of the *E. coli* and *S. typhimurium* experiments, we obtain the mathematical model in dimensionless form

$$\begin{aligned}\frac{\partial n}{\partial t} &= D_n\nabla^2 n - \alpha\nabla\left[\frac{n}{(1+c)^2}\nabla c\right] + \rho n\left(\delta\frac{s^2}{1+s^2} - n\right)\\ \frac{\partial c}{\partial t} &= D_c\nabla^2 c + \beta\, s\,\frac{n^2}{\gamma+n^2} - nc\\ \frac{\partial s}{\partial t} &= D_s\nabla^2 s - \kappa n\frac{s^2}{1+s^2}\ .\end{aligned} \tag{2}$$

The quantity ∇^2 represents the Laplacian in two space dimensions, and α, β, γ, δ, ρ, κ are parameters. The reader is referred to [25,23,24] for more detail concerning solutions admitted by the model and mathematical analysis of the equations.

3. Numerical methods

Chemotaxis models have been studied for some time, both numerically and analytically. Many of the early models of *E. coli* patterns had analytic solutions available, since diffusion of the chemoattractant/food was assumed so small as to be negligible [6,8]. For more complex models, a straightforward method such as Crank-Nicholson applied to the whole model (as described below) with Successive Over-Relaxation (SOR) iterations has been used successfully [28]. Other researchers did simulations in one dimension [17,20], which is a much easier problem. Those researchers interested in two dimensional patterns were looking at steady state patterns on relatively small domains [15,28]. Recently, a number of other numerical methods have been used to obtain interesting pattern formation results [3,4], but unfortunately the numerical methods are not explored in the literature.

The *E. coli* and *S. typhimurium* model (2) is a challenging one numerically for a number of reasons. Of these, the highly nonlinear chemotaxis and reaction terms are immediately apparent. In addition, the model contains diffusion terms which have infinite propagation speeds in the context of solutions. As mentioned above, the interaction between the chemotaxis and diffusion terms is a fundamental part of the pattern-forming process, and so neither can be ignored. For the model system (2), the parameter values are such that diffusion and chemotaxis are equally important. In addition, this modelling project is particularly difficult because ultimately, patterns are sought on large domains across which a disturbance must propagate for some time without hitting the far boundary. We are thus motivated to find a computationally efficient method which allows us to maximise the spatial and temporal grid spacing. The method presented here has the potential to substantially reduce the computational effort required to solve chemotaxis equations.

As chemotaxis models become more nonlinear and increasingly difficult to analyse, particularly close attention needs to be paid to the numerical methods used in their study. Research on chemotaxis equations tends to focus on parameter domains where the equations are locally linearly unstable, which makes appropriate choice and use of numerical methods especially important.

One approach to solving the system of equations (2) is to model all terms simultaneously, replacing each of the derivatives by finite differences and marching forward in time. Such a method will typically need to be implicit because of the diffusion terms, which otherwise would cause a severe time step restriction. See, for example, [16, 22] for general discussion of standard numerical methods and issues. The reaction terms may also contribute to the necessity of using an implicit method if some fast reactions reach equilibrium on a much faster time scale than the processes being modeled (*i.e.*, if the reaction terms are "stiff"). A second-order accurate implicit method is easily obtained by using a trapezoidal rule discretisation in time and centered differences in space (as in the standard Crank-Nicolson method for the pure diffusion or heat equation). This leads to a method in which all terms, including the advective terms, are implicit and centered in space, and in which there is nonlinear coupling between all components at all grid points.

The chemotaxis term taken alone however, can be viewed as advective and thus hyperbolic in character. Such terms can typically be handled best by explicit methods. Making these highly nonlinear terms implicit can lead to difficulties in solving the implicit system in each time step. Moreover, using centered approximations can lead to well-known difficulties with nonphysical oscillations arising near discontinuities or steep gradients in the solution [11]. For pattern formation problems we expect spots or stripes with steep gradients to form, and it is critical that we resolve these well.

Excellent explicit methods have been developed for hyperbolic systems of conservation laws with discontinuous solutions, largely in the context of gas dynamics in aerodynamics and astrophysics, where shock waves are a prominent feature. These "high-resolution" methods are second order accurate in regions where the solution is smooth and also give sharp resolution of discontinuities or steep gradients. A general introduction can be found in [11]. These methods can be adapted for solving advection equations of the type that arise in chemotaxis, and in this

work the software package CLAWPACK (Conservation LAWs PACKage) is used, as described in the next section.

In order to take advantage of these methods for advective terms, it is easiest to use a fractional step method. We refer specifically to one in which the solution procedure is split up into independent steps corresponding to the advection, diffusion, and reaction processes, and each step is handled independently. This allows us to isolate the chemotaxis term from the Fickian diffusion and reaction terms, and thus to treat it as an advection term. We can write the full system of equations in the form

$$q_t = \mathscr{D}(q) + \mathscr{A}(q) + \mathscr{R}(q) \tag{3}$$

where $q = (u, v, w)$ is the vector of unknowns, $\mathscr{D}(q)$ represents the diffusive terms in the equation, $\mathscr{A}(q)$ the advection terms, and $\mathscr{R}(q)$ the reaction terms. If q^n is the solution at time t_n, then in the simplest fractional step method we would update q^n to obtain q^{n+1} at time $t_{n+1} = t_n + \Delta t$ in a sequence of three steps:

1. Solve $q_t = \mathscr{A}(q)$ over time Δt with data q^n to obtain q^*,
2. Solve $q_t = \mathscr{D}(q)$ over time Δt with data q^* to obtain q^{**},
3. Solve $q_t = \mathscr{R}(q)$ over time Δt with data q^{**} to obtain q^{n+1}.

We can abbreviate this procedure as $q^{n+1} = R(\Delta t)D(\Delta t)A(\Delta t)q^n$. It can be shown that this results in a first order accurate approximation for the full equations. Moreover, if we use the "Strang splitting" we can obtain second order accuracy, provided each subproblem is solved with a second order accurate method [21]. The Strang splitting is a symmetric version of the above procedure of the form

$$q^{n+1} = A(\Delta t/2)D(\Delta t/2)R(\Delta t)D(\Delta t/2)A(\Delta t/2)q^n.$$

For general discussions of fractional step methods, see for example [22, 27].

The advantage of a fractional step method is that we can use the most suitable method for each problem independently, such as the high-resolution methods for advection mentioned above. In Sections 5 and 6 we discuss the methods of choice for the reaction and diffusion steps, and in Section 7 we present some numerical results for the chemotaxis equations of Section 2. In Section 8 we give some discussion of a stability problem that was found in using the standard Crank-Nicolson method for the diffusion step, which would seem to be a natural choice. This motivates the need for the TR-BDF2 method advocated in Section 6.

4. The advection step

For the advection step, we use the CLAWPACK algorithms described in [13]. The algorithms are too complicated to present in detail here, and the original paper [13] should be consulted for complete information. The special case of advection in a divergence-free velocity field is described in detail in [12]. This arises when advecting a quantity in an incompressible fluid flow, for example, in which case the fluid density is constant and consequently the velocities u and v (in two dimensions) satisfy $u_x + v_y = 0$. The velocity fields we must consider here are not

divergence-free, and indeed the pattern formation we hope to model is dependent on cells clustering together in some regions. The advection equation has the form

$$n_t + (un)_x + (vn)_y = 0, \tag{4}$$

where the velocity field is defined by

$$u = \frac{\alpha}{(1+c)^2}\frac{\partial c}{\partial x} \tag{5}$$

$$v = \frac{\alpha}{(1+c)^2}\frac{\partial c}{\partial y} \tag{6}$$

We use a finite-volume method in which n_{ij} represents the average of n over the (i, j) grid cell of size $\Delta x \Delta y$. (Note: grid cells should not be confused with biological cells!) To update the cell average of n, the algorithm of [13] requires that we solve the "Riemann problem" at each interface between grid cells. This is simply the one-dimensional equation normal to the interface with piecewise constant data defined by the values in each adjacent cell. For example, consider the interface between cells $(i-1, j)$ and (i, j). We must solve $n_t + (un)_x = 0$ with data $n_{i-1,j}$ and n_{ij}. For the scalar advection equation this results in a wave of strength

$$\mathscr{W} = n_{ij} - n_{i-1,j}$$

propagating at some speed $u_{i-1/2,j}$. Based on (5), we define this speed by

$$u_{i-1/2,j} = \frac{\alpha}{(1+c_{i-1/2,j})^2}\left(\frac{c_{ij} - c_{i-1,j}}{\Delta x}\right), \tag{7}$$

where $c_{i-1/2,j}$ is an average value of c,

$$c_{i-1/2,j} = \frac{c_i + c_{i-1}}{2}$$

The algorithm also requires that we compute a flux-difference splitting of the jump in un between the two cells into left-going and right-going flux-differences, denoted by $\mathscr{A}^-\Delta q$ and $\mathscr{A}^+\Delta q$. Following CLAWPACK Note #8 [10], we define these by

$$\mathscr{A}^-\Delta q = F_{i-1/2,j} - u_{i-1,j}n_{i-1,j}$$
$$\mathscr{A}^+\Delta q = u_{ij}n_{ij} - F_{i-1/2,j}$$

where

$$F_{i-1/2,j} = \begin{cases} u_{i-1/2,j}n_{i-1,j} & \text{if } u_{i-1/2,j} \geq 0 \\ u_{i-1/2,j}n_{i,j} & \text{if } u_{i-1/2,j} < 0 \end{cases}$$
$$u_{ij} = \max(u_{i-1/2,j}, 0) + \min(u_{i+1/2,j}, 0).$$

We must also define the manner in which these flux-differences move in the transverse direction, *i.e.* a splitting of $\mathscr{A}^+\Delta q$ into $\mathscr{B}^-\mathscr{A}^+\Delta q_{ij}$ and $\mathscr{B}^+\mathscr{A}^+\Delta q_{ij}$, and

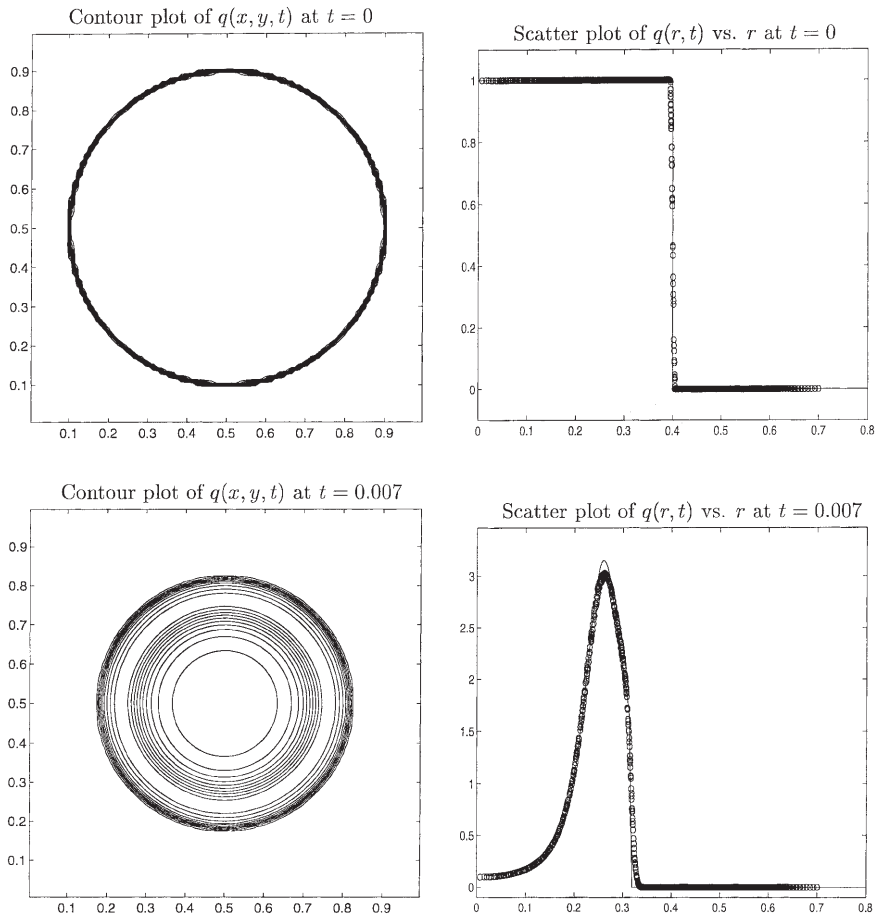

Fig. 1. Computed results for the test problem of Section 4.

similarly for $\mathscr{A}^- \Delta q$ (in the notation of [13]). This is accomplished by

$$\mathscr{B}^+ \mathscr{A}^\pm \Delta q^1 = \max(v_{i,j+1/2}, 0) \mathscr{A}^\pm \Delta q^1$$
$$\mathscr{B}^- \mathscr{A}^\pm \Delta q^1 = \min(v_{i,j-1/2}, 0) \mathscr{A}^\pm \Delta q^1$$

where, for example, $v_{i,j-1/2}$ is the velocity normal to the interface between cells $(i, j-1)$ and (i, j) and is defined following (6) by

$$v_{i,j-1/2} = \frac{\alpha}{(1 + c_{i-1/2,j})^2} \left(\frac{c_{ij} - c_{i,j-1}}{\Delta y} \right). \tag{8}$$

These formulas are encoded in the Riemann-solvers `rpn2` and `rpt2` required by CLAWPACK, which then implements the algorithm of [13] to give a "high-resolution" solution that is second-order accurate where n is smooth and that uses

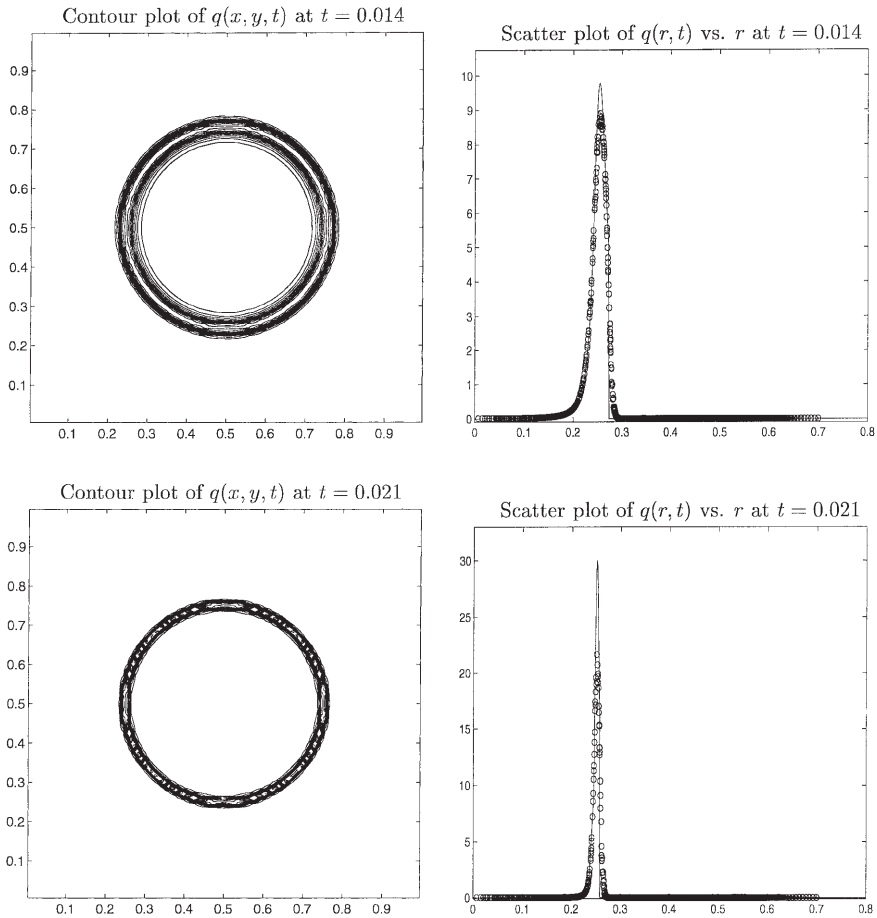

Fig. 1. (continued)

"flux-limiters" to maintain sharp resolution of discontinuities or steep gradients with minimal smearing or nonphysical oscillation.

As an example to show that this advection algorithm is effective for the type of problems arising in chemotaxis, we present one test case where we simply advect a scalar quantity up the gradient of a chemoattractant with a fixed density profile. On the unit square we set

$$c(x, y) = 1 - \cos(4\pi r(x, y)) \tag{9}$$

for all t, where

$$r(x, y) = \sqrt{(x - 0.5)^2 + (y - 0.5)^2}$$

is the distance from the center. This gives a ring of chemoattractant with maximum at $r = 0.25$. The velocity profile is given by ∇c and computationally we use

velocities analogous to (7) and (8) based on differencing this function c between grid cells.

We initialize n to be 1 inside a circle of radius 0.4 about the center and 0 outside (so that boundary conditions do not affect the solution). This corresponds to a uniform lawn of cells inside this disk, which then move up the chemoattractant's gradient and tend to cluster into a ridge about $r = 0.25$. This problem was solved on a 100×100 grid with time step $\Delta t \approx 0.0072$ corresponding to a Courant number of 0.9.

Figure 1 shows contour plots of the computed n at several times. At each time we also show a scatter plot of all the 10,000 solution values q_{ij} plotted against $r(x_i, y_j)$, the distance of the grid point from the center. Since the solution should be radially symmetric, all of these points should lie on a curve $\tilde{q}^1(r, t)$. The solid line in these figures is this true solution $\tilde{q}^1(r, t)$, as obtained by solving the reduced one-dimensional equation

$$\tilde{q}^1_t + U(r)\tilde{q}^1_r = -(U(r)/r + U'(r))\tilde{q}^1$$

by the method of characteristics with an accurate ODE solver. Here $U(r)$ is the velocity in the r direction, found by differentiating c from (9) with respect to r.

We see that the solution remains highly symmetric in spite of the fact that a Cartesian grid is used. There is very little scatter of points near any fixed value of r, indicating that the method is quite isotropic and shows little grid-orientation effects. This is very important for the pattern formation studied here, since the break-up of rings into spots seen in Section 7 could easily be affected by numerical artifacts.

We also see that there is little loss of resolution in the numerical solution until times at which the ridge of n is too narrow to be resolved on this particular grid. By contrast, a first-order method (*e.g.*, upwind) would produce a more smeared solution, while a standard second-order methods such as Lax-Wendroff would produce oscillations and undershoots near the edge of the ridge, giving rise to nonphysical negative cell densities. In these computations, where the van Leer limiter has been used, there are some very slight undershoots, on the order of 10^{-4} at most.

It is also important to note that this method is completely conservative. Even at the last time shown, when the ridge is not very well resolved, the total mass of cells present (measured by $\Delta x \Delta y \sum n_{ij}$) is conserved to machine precision.

5. The reaction step

The reaction step consists of solving a coupled system of ordinary differential equations in each grid cell. Selecting the reaction terms in (2) we obtain the system of equations

$$\begin{aligned}
\frac{\partial n}{\partial t} &= \rho n \left(\delta \frac{s^2}{1+s^2} - n \right) \\
\frac{\partial c}{\partial t} &= \beta s \left(\frac{n^2}{\gamma + n^2} \right) - nc \\
\frac{\partial s}{\partial t} &= -\kappa n \left(\frac{s^2}{1+s^2} \right) .
\end{aligned} \tag{10}$$

There are no spatial derivatives and hence no spatial coupling of different grid cells in this step. This is another advantage of the fractional step approach: if we use an implicit method, which may be necessary for stability reasons on some problems, then we obtain decoupled small systems of equations at each grid point, rather than a large system coupling together all grid points. Since the reaction terms may be highly nonlinear, this decoupling of the reaction terms from spatial derivatives is advantageous.

For the problems studied here, we have found that the method chosen for the reaction terms has little impact on the solution obtained. The fourth-order explicit Runge-Kutta method and the first-order implicit backward Euler method, two radically different methods, have both been tried with essentially the same results.

Note that a 1-step method must be used, rather than a linear multi-step method, since data from previous time steps is not available when the reaction equations are solved. As a general recommendation, a second-order implicit method is most reliable for the reaction step. The trapezoidal rule (TR) may be a reasonable choice for many problems, since it is A-stable [7], meaning that it behaves properly on the test equation $q' = \lambda q$ when $\mathrm{Re}(\lambda) < 0$ and the true solution decays exponentially. An A-stable method gives a decaying numerical solution for any size time step Δt. This is particularly important if the problem is stiff, meaning that we wish to use a time step Δt that is large compared to some time scales λ^{-1} in the problem, *i.e.*, $\lambda \Delta t$ is large in magnitude. This could occur if the fast time scales are essentially in equilibrium and we are not attempting to track transient behaviour on this time scale.

In the fractional step method, however, it is possible that these terms will be thrown out of equilibrium in other steps of the process. In this case we would like the method used in the reaction step to restore equilibrium. For the test equation, this means we would like $q^{n+1} \to 0$ as $\lambda \Delta t \to -\infty$ regardless of the value of q^n. A method with this property is called L-stable [7].

The TR method is not L-stable, and instead $q^{n+1} \to -q^n$ as $\lambda \Delta t \to -\infty$. The method remains stable in this limit, but produces oscillatory solutions. Exactly this problem is seen in the diffusion step if the Crank-Nicolson method (which is based on TR) is used, as discussed in Section 6 and Section 8.

One possible alternative method is the TR-BDF2 method [2], an implicit Runge-Kutta method based on taking a time step of length $\gamma \Delta t$ where $\gamma < 1$ with TR to obtain an intermediate value $q^{n+\gamma}$, and then using the 2-step BDF method on q^n and $q^{n+\gamma}$ to obtain q^{n+1}. The value $\gamma = 2 - \sqrt{(}2) \approx 0.59$ gives the minimum error and makes it possible to use an efficient approximate-Newton iteration, but very little accuracy is lost by using $\gamma = 1/2$. Since the latter value is simpler to use in our formulation, we assume that value for the remainder of the paper. On the ordinary differential equation $q_t = \mathscr{R}(q)$ the method thus has the form

$$q^{n+1/2} = q^n + \frac{\Delta t}{4}\Big(\mathscr{R}(q^n) + \mathscr{R}(q^{n+1/2})\Big), \tag{11}$$

$$q^{n+1} = \frac{1}{3}\Big(- q^n + 4q^{n+1/2} + \Delta t \mathscr{R}(q^{n+1})\Big). \tag{12}$$

This method is both A-stable and L-stable, and second-order accurate.

In the problems considered here, the reaction terms are not stiff and, as noted above, we have not needed such a method in the reaction step. (This method is crucial however, for the diffusion step discussed in the next section.) We have not experimented with chemotaxis problems having stiff reaction terms, but it is worth noting that for problems where there are fast transients occurring only within some "reaction front", it may be necessary to use sufficiently small time steps that will resolve these fast transients rather than relying on an implicit method such as TR-BDF2. The coupling between the reaction step and the other processes is known to cause numerical difficulties such as reaction fronts that travel at incorrect speeds. This has been observed in combustion problems, for example, and is analyzed for a simple model problem in [14].

6. The diffusion step

The diffusion equations take the form

$$n_t = D_1 \nabla^2 n, \qquad c_t = D_2 \nabla^2 c, \qquad s_t = D_3 \nabla^2 s \ .$$

Each of these is simply the linear diffusion equation on each component. For numerical solutions, the standard second-order accurate Crank-Nicolson method would be a natural choice. This is just the trapezoidal rule from the previous section applied to the system of ordinary differential equations obtained by replacing the Laplacian operator Δ^2 by the discrete operator

$$\nabla_h^2 q_{ij} = \frac{1}{h^2}(q_{i-1,j} + q_{i+1,j} + q_{i,j-1} + q_{i,j+1} - 4q_{ij})$$

where $q = (n, c, s)$. This approach has proved satisfactory in studying the propagation of swarm rings. The performance of the method on the *E. coli* and *S. typhimurium* model (2) however, is entirely different when we seek stationary patterns, like those obtained by *S. typhimurium*. If we try to obtain numerical solutions for Courant numbers close to 1, the simulations rapidly develop grid scale oscillations that are not adequately damped by the Crank-Nicolson method. The numerical method does not become stable until the timestep is drastically reduced, requiring Courant numbers less than 0.01. At such small values the method is very slow and, more importantly, the advective step becomes maximally diffusive. This instability results from the fact that TR is not L-stable. Grid-scale oscillations arising from the nonlinear interaction of the advection and reaction steps should be damped by the diffusion step, but with Crank-Nicolson these oscillations are instead negated as discussed in Section 5 and grow worse in subsequent steps. This is analyzed in more detail in Section 8.

Instead we have used the TR-BDF2 method (11) for the diffusion steps and obtained good results. Note that each stage of this 2-stage method now requires solving a large linear system of equations coupling together all grid points. However, unlike the reaction terms, these equations are linear. Also, the equations for n, c, and s are decoupled from one another.

We implemented TR-BDF2 by splitting the method dimensionally and then correcting for cross terms by using a few sweeps of Gauss-Seidel (or under-relaxed

Jacobi) iteration. The first stage of the method, TR, is implemented by taking one step of a locally one-dimensional (LOD) method, which is just a fractional step method in which the x- and y-derivative terms are split apart, resulting in simple tridiagonal systems of equations to solve along each grid line [22]. The second stage, BDF2, is implemented first by taking another step of an LOD method, with different coefficients this time. This gives a very good initial guess for the Gauss-Seidel procedure. In principle advancing by LOD alone should be enough to maintain second order accuracy, but we have found that this can reintroduce grid-scale oscillations that cause stability problems of the sort described in Section 8, and so the Gauss-Seidel sweeps are used to damp these high-frequency oscillations.

7. Numerical results

Numerical simulation results compare well with the patterns obtained experimentally. The continuous and spotted concentric ring patterns of Figures 2 and 3 compare well with the *S. typhimurium* experiments, and the radial spots pattern of Figure 4 is very similar to the radial spots pattern observed in some of the *E. coli* experiments. In addition, the temporal sequence of events leading to the formation of the numerical patterns is the same as that reported experimentally in the two cases (*E. coli* and *S. typhimurium*). That is, for *S. typhimurium* we see a low density bacterial lawn spread out discwise from the initial inoculum, followed by the formation of continuous or spotted concentric rings within the lawn. For *E. coli* we see the formation of a high cell density swarm ring which sheds a regular pattern of spots in its wake.

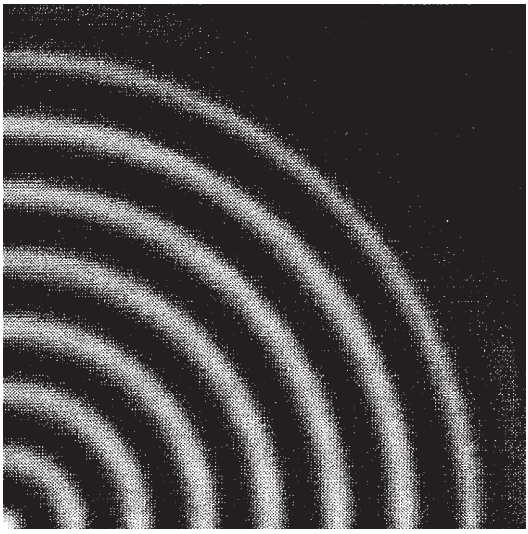

Fig. 2. Simulation results for the semi-solid medium model showing a *S. typhimurium* pattern of concentric rings. White indicates high cell density, black the opposite. Parameter values: $d_n = 0.25$, $d_s = 1.0$, $\alpha = 2.25$, $\beta = 0.2$, $\delta = 20$, $\rho = 0.01$, $\kappa = 0$, $\mu = 1$ and $s = 1$. Simulation Parameters: $\Delta x = 0.08$, $\Delta t = 0.03$.

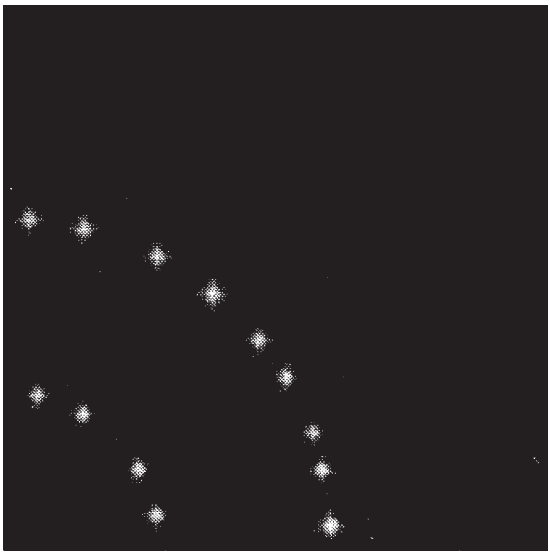

Fig. 3. Simulation results for the semi-solid medium model showing a *S. typhimurium* pattern of concentric spotted rings. White indicates high cell density, black the opposite. Parameter values: $d_n = 0.25$, $d_s = 1.0$, $\alpha = 5$, $\beta = 0.2$, $\delta = 20$, $\rho = 0.01$, $\kappa = 0$, $\mu = 1$ and $s = 1$. Simulation Parameters: $\Delta x = 0.3$, $\Delta t = 0.01$.

The pattern elements are very distinct from the surrounding regions as is shown in a surface plot (Figure 5). Grid refinement studies were carried out for simulations in one dimension to verify that the solutions obtained are real. The effect of the boundary was also checked by running the two dimensional simulations on a large domain with the initial inoculum of cells placed at the centre. The simulation shows that boundary effects are not triggering the formation of the observed pattern (Figure 6). Finally, a nonlinear analysis was carried out on the model equations [23], and the numerical results compared with the analytic solutions. The grid spacing and timestep interval used for each figure is indicated in the figure caption.

8. A numerical instability

We mentioned earlier that it is necessary to use a method which is both A-stable and L-stable for the diffusion step in order to prevent grid-scale oscillations from developing. Difficulties with methods which have very slow decay of high frequency solution modes has been observed previously in the context of reaction-diffusion equations [19] and reaction-convection-diffusion equations [1]. In our reaction-chemotaxis-diffusion model the problem is even more severe due to the nonlinear nature of the chemotaxis term.

To investigate the nature of this instability, we consider a very simplified version of the model (2) with a minimum number of terms and nonlinearities

$$\frac{\partial n}{\partial t} = D_n \nabla^2 n - \alpha \nabla (n \nabla c)$$

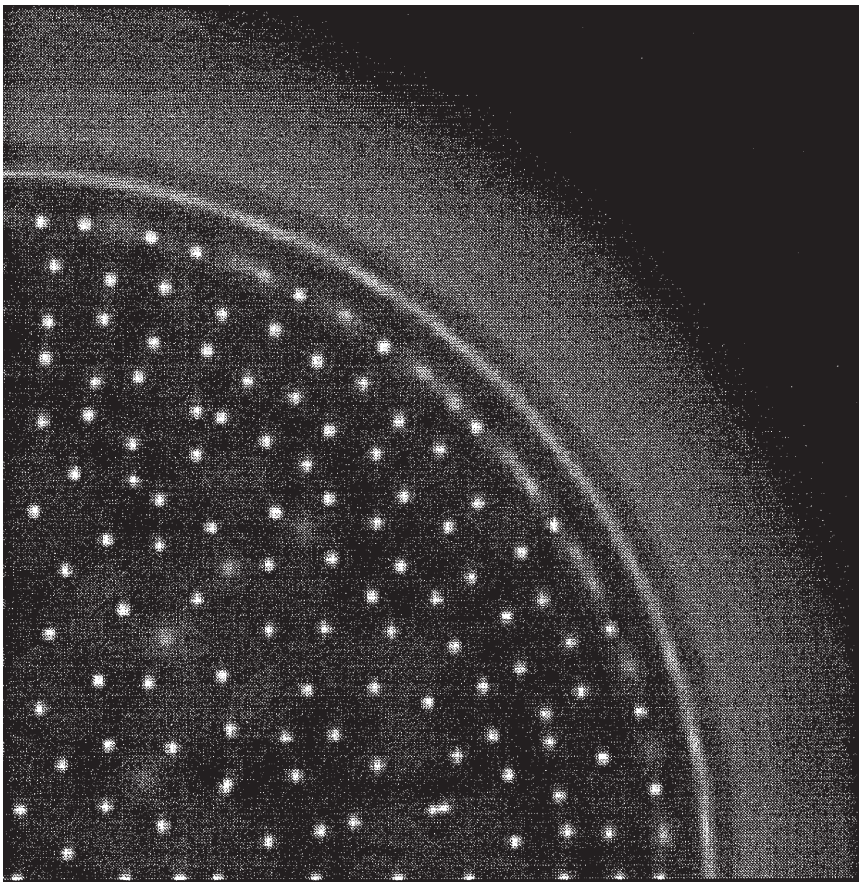

Fig. 4. Simulation result showing a radial spots pattern left behind an expanding swarm ring. Parameter values: $d_n = 0.25$, $d_s = 1.0$, $\alpha = 35$, $\beta = 6$, $\delta = 3.5$, $\rho = 1$, $\kappa = 0$, $\mu = 100$ and $s = 1$. Simulation Parameters: $\Delta x = 0.14$, $\Delta t = 0.01$.

$$\frac{\partial c}{\partial t} = D_c \nabla^2 c - nc \ . \tag{13}$$

In this model the cells and chemoattractant both diffuse, the cells are advected up the chemoattractant gradient (chemotaxis), and the cells consume the chemoattractant.

It is difficult to do a theoretical stability analysis of this model, due to the fact that it is the nonlinear interaction of the chemotaxis and diffusion terms, coupled with the reaction terms (also highly nonlinear) which is fundamental to the pattern-forming process. Any analysis of the model and method must embrace that nonlinearity; therefore we investigate the solution stability numerically.

When tested individually on the appropriate portions of the model (13), each step in the Strang splitting procedure is stable for reasonable timestep intervals. When tested in pairs however, the advection-diffusion and reaction-diffusion pairings are stable while the advection-reaction pairing is highly unstable. The reaction

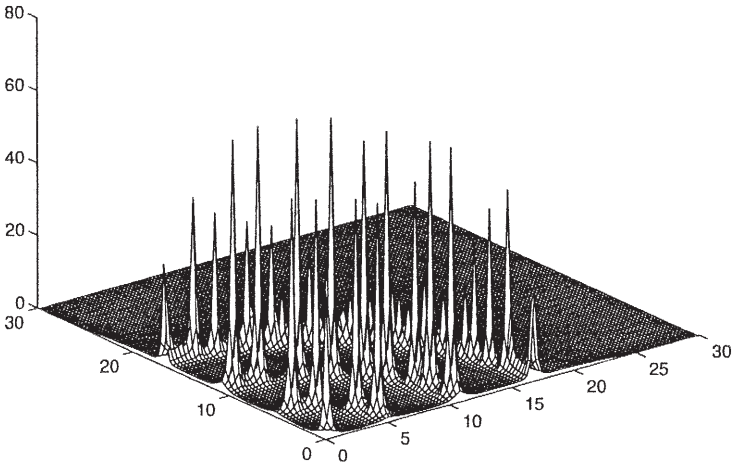

Fig. 5. Surface plot of the cell density distribution in a *S. typhimurium* pattern. Parameter values: $d_n = 0.25$, $d_s = 1.0$, $\alpha = 5$, $\beta = 0.2$, $\delta = 20$, $\rho = 0.01$, $\kappa = 0$, $\mu = 1$ and $s = 1$. Simulation Parameters: $\Delta x = 0.3$, $\Delta t = 0.01$.

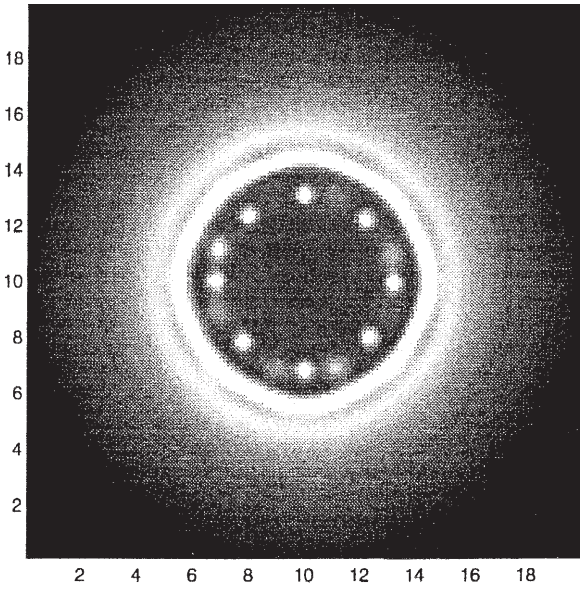

Fig. 6. Swarm ring pattern centred in the domain. Parameter Values: $d_n = 0.25$, $d_s = 1.0$, $\alpha = 90$, $\beta = 10$, $\delta = 6.6$, $\rho = 1$, $\kappa = 0.5$ and $s = 1.0$. Simulation Parameters: $\Delta x = 0.14$, $\Delta t \leq 0.01$.

terms (here just the consumption of chemoattractant by the cells) change the chemoattractant concentration and therefore the surface over which the cells advect. This coupling is numerically observed to be unstable (Fig. 7).

Physically, the presence of diffusion in the system should damp high frequency oscillations. When the full model is solved numerically however, the timestep

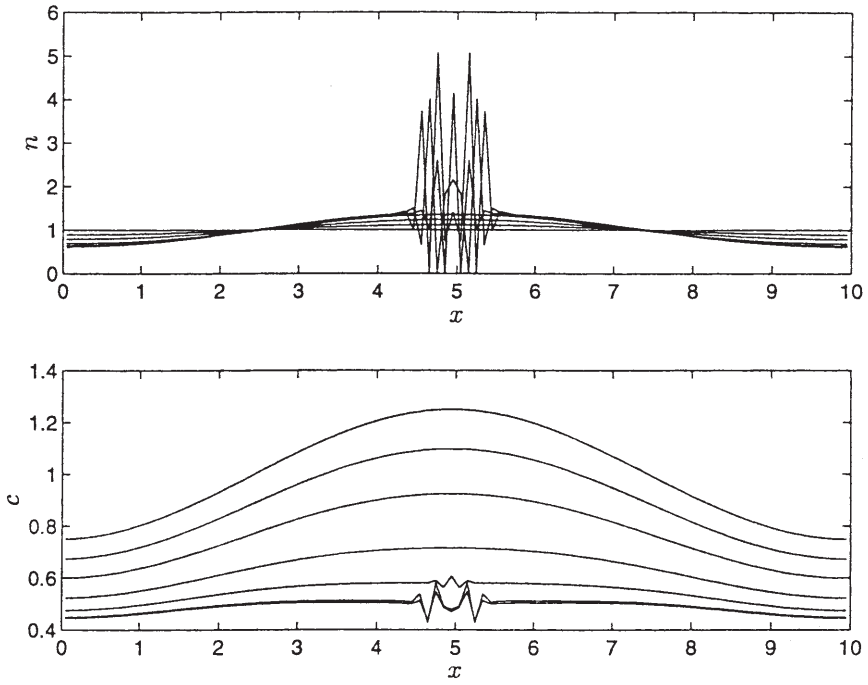

Fig. 7. Simulation result showing instability developing in the solution of model (13) when the advection and reaction portions are run alone. Cell density (n) and chemoattractant concentration (c) are plotted against x at various timesteps. The grid scale noise appears to arise in connection with the chemoattractant profile flattening and changing concavity. The results are plotted at several different times to show the instability developing. In the cell density plot, the curves increase in concavity as time increases. In the chemoattractant concentration plot, the curves decrease in concavity as time increases. Simulation Parameters: $\Delta x = 0.1$, $\Delta t = 0.5$.

required to prevent high frequency oscillations from overwhelming the results is very small when the diffusion term is discretised according to the Crank-Nicolson formula. A much larger timestep is possible when the diffusion term is discretised according to the TR-BDF2 formula, which is far more effective at damping high frequency oscillations. The two methods in one dimension are compared in Figure 8. The same conclusions apply to the full model (2) and are illustrated in Figure 9.

For models in which the two diffusion coefficients are very different in magnitude the Crank-Nicolson method can be particularly troublesome. Consider for example the situation $D_n \gg D_c$. Then the diffusion of the chemoattractant can be ignored in the short term. To see how a grid-scale oscillation can grow, suppose we start with constant c and n and introduce a small amplitude grid-scale oscillation, alternating positive and negative at adjacent grid points. The cells are attracted up the resulting gradient so that after the advection step the density n will have the same oscillatory pattern. The diffusion step should now damp these oscillations, but if we use Crank-Nicolson with a timestep for which $\Delta t D_n / \Delta x$ is large then the oscillations in n will be essentially negated rather than damped, as discussed in

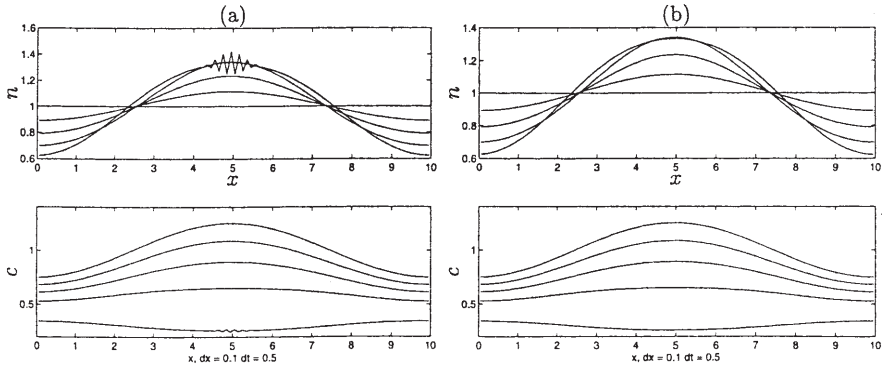

Fig. 8. Simulation result showing the effect of adding diffusion to the model. Compare with the advection-reaction pairing shown in Figure 7. Cell density (n) and chemoattractant concentration (c) are plotted against x at various timesteps. Crank-Nicolson diffusion (a) doesn't sufficiently dissipate the high frequencies to prevent grid scale noise from appearing in the solution. TR-BDF2 diffusion (b) does provide sufficient diffusivity. The results are plotted at several different times to show the instability developing. In the cell density plot, the curves increase in concavity as time increases. In the chemoattractant concentration plot, the curves decrease in concavity as time increases. Simulation Parameters: $\Delta x = 0.1$, $\Delta t = 0.5$.

Section 5. As a result, n is now *larger* at the grid points where c is smaller; the cells have clustered where there is *less* chemoattractant. In the reaction step the cells thus eat more chemoattractant at these points than where c is larger, leading to an amplification of the oscillation. This can grow in an unstable manner in subsequent time steps.

Our findings confirm the trend observed in other numerical methods for parabolic partial differential equations, namely that it is important to use a method which is both A-stable and L-stable. We investigated changing the methods used for the reaction and advection steps, but these did not eliminate the problem. Closer examination of the coupling between the various steps in the Strang splitting procedure should reveal exactly how the grid scale noise arises.

9. Conclusions

We present in this paper a numerical method for solving nonlinear reaction-diffusion-chemotaxis equations which arise in models for biological systems. The numerical method is straightforward to implement and produces good results. With the splitting approach we can take advantage of the most sophisticated methods available for each component of the model. We thus obtain a combined method which is potentially much faster than a method which involves solution of the entire system of equations and nonlinear iteration at each timestep.

Consistent with results reported by other research in numerical analysis, we find that it is necessary to use methods which are effective at damping high frequency oscillations in order to have a stable numerical method at a reasonable timestep size. This adds further evidence that the widely used Crank-Nicolson method should be applied with care. The tendency of the model (2) to amplify high frequency

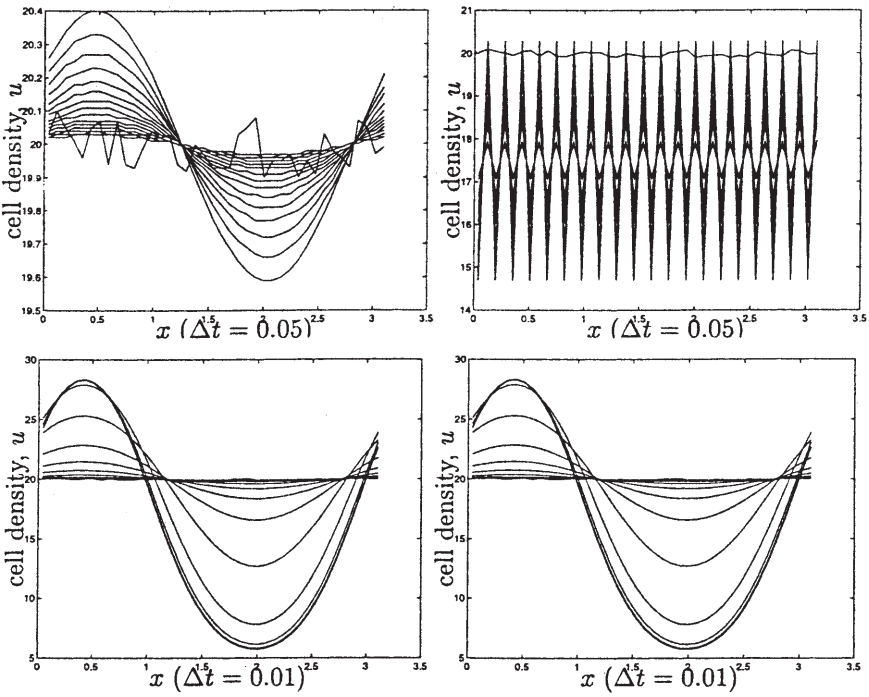

Fig. 9. Comparison of the method with TR-BDF2 diffusion (left column) and with Crank Nicholson diffusion (right column) on the model equations (2). All solutions shown were run to $t = 300$ or steady state, whichever came first. From top to bottom, Δt is decreased (0.05, 0.01), $\Delta x = 0.08$ is held constant. Parameter values: $D = 0.25$, $\alpha = 2.25$, $\beta = 0.2$, $\beta_2 = -0.01$, $\mu = 1.0$, $\delta = 20.0$, $\rho = 0.01$, $w = 1.0$, $u_0 = u^* = 20.0$, $v_0 = v^* = 4.0$, $k_c^2 = 4.0$ and $l_x = l_y = l = 3.1416$ (domain which can sustain one 2π oscillation). Solutions at several different times are presented to show the evolution of the solution from the randomly perturbed uniform initial condition to the sinusoidal solution or grid scale noise. The initial condition in each case is the same, but the ordinate scale is different between the top and bottom plots.

oscillations is here further exacerbated by the splitting of the model into separate consecutive components. We use the two stage method TR-BDF2 for the diffusion step, and propose that this, or a similarly L-stable method, could be used for the reaction step in cases where those terms are very stiff.

The manner in which we split the model into components allowed for the greatest simplification of each portion of the numerical method. Other splitting choices could be made however, and these will be investigated in future work. To our knowledge, this work represents the first time the high resolution advection scheme, CLAWPACK, has been used to numerically solve a reaction-diffusion-chemotaxis equation. Previously, useful numerical results have been obtained with a first order Riemann solver advection scheme [18]. We have here used CLAWPACK, which is a second order method, and the good quality of the results indicates that this software should be generally useful for models involving chemotaxis.

Acknowledgements. This work was supported in part by (RT) NSERC awards PGSA and PGSB, (LGS and RJL) DOE grant DE-FG03-96ER25292 and NSF grants DMS-9626645 and DMS-9505021.

References

[1] Ascher, U., Ruuth, S., Wetton, B.: Implicit-explicit methods for time-dependent partial differential equations, SIAM Journal of Numerical Analysis, **32**, 797–823 (1995)
[2] Bank, R., Coughran, W.J., Fichtner, W., Grosse, E., Rose, D., Smith, R.: Transient simulation of silicon devices and circuits, IEEE Transactions on Computer-Aided Design, 436–451 (1985)
[3] Ben-Jacob, E., Cohen, I., Shochet, O., Aranson, I., Levine, H., Tsimring, L.: Complex bacterial patterns, Nature, **373**, 566–567 (1995)
[4] Bruno, W.: Patterns that grow, CNLS Newsletter, **82**, 1–10 (1992)
[5] Budrene, E., Berg, H.: Complex patterns formed by motile cells of escherichia coli, Nature, **349**, 630–633 (1991)
[6] Keller, E., Segel, L.: Model for chemotaxis., Jour. Theor. Biol., **30**, 225–234 (1971a)
[7] Lambert, J.D.: Computational Methods in Ordinary Differential Equations, Wiley, 1973
[8] Lauffenburger, D., Kennedy, C., Aris, R.: Traveling bands of chemotactic bacteria in the context of population growth, Bull. Math. Biol., **46**, 19–40 (1984)
[9] LeVeque, R.J.: CLAWPACK software. available from `netlib.att.com` in `netlib/pdes/claw` or on the Web at the URL `http://www.amath.washington.edu/~rjl/clawpack.html`
[10] LeVeque, R.J.: CLAWPACK User Notes. available from `netlib.bell-labs.com` in `netlib/pdes/claw/doc` or at `http://www.amath.washington.edu/~rjl/clawpack.html`
[11] LeVeque, R.J.: Numerical Methods for Conservation Laws, Birkhäuser-Verlag, 1990
[12] LeVeque, R.J.: High-resolution conservative algorithms for advection in incompressible flow, SIAM J. Numer. Anal., **33**, 627–665 (1996)
[13] LeVeque, R.J.: Wave propagation algorithms for multi-dimensional hyperbolic systems, J. Comput. Phys., **131**, 327–353 (1997)
[14] LeVeque, R.J., Yee, H.C.: A study of numerical methods for hyperbolic conservation laws with stiff source terms, J. Comput. Phys., **86**, 187–210 (1990)
[15] Maini, P., Myerscough, M., Winters, K., Murray, J.: Bifurcating spatially heterogeneous solutions in a chemotaxis model for biological pattern generation, Bull. Math. Biol., **53**, 701–719 (1991)
[16] Mitchell, A.R., Griffiths, D.F.: The Finite Difference Method in Partial Differential Equations, Wiley, 1980
[17] Myerscough, M., Murray, J.: Analysis of a propagating pattern in a chemotaxis system., Bull. Math. Biol., **54**, 77–94 (1992)
[18] Rascle, M., Ziti, C.: Finite time blow-up in some models of chemotaxis, Journal of Mathematical Biology, **33**, 388–414 (1995)
[19] Ruuth, S.: Implicit-explicit methods for reaction-diffusion problems in pattern formation, Journal of Mathematical Biology, **34**, 148–176 (1995)
[20] Scribner, T., Segel, L., Rogers, E.: A numerical study of the formation and propagation of traveling bands of chemotactic bacteris, J. Theor. Biol., **46**, 189–219 (1974)
[21] Strang, G.: On the construction and comparison of difference schemes, SIAM J. Num. Anal., **5**, 506–517 (1968)
[22] Strikwerda, J.C.: Finite Difference Schemes and Partial Differential Equations, Wadsworth & Brooks/Cole, 1989

[23] Tyson, R.C.: Pattern Formation by E. coli and S. typhimurium – Mathematical and Numerical Investigation of a Biological Phenomenon, PhD thesis, University of Washington, 1996
[24] Tyson, R., Lubkin, S., Murray, J.: Model and analysis of chemotactic bacterial patterns in a liquid medium, J. Math. Biol. **38**, 359–375 (1999)
[25] Tyson, R., Lubkin, S., Murray, J.: A minimal mechanism of bacterial pattern formation. Proc. Roy. Soc. Lond. **B266**, 299–304 (1998)
[26] Woodward, D., Tyson, R., Myerscough, M., Murray, J., Budrene, E., Berg, H.: Spatio-temporal patterns generated by S. typhimurium, Biophysical Journal, **68**, 2181–2189 (1995)
[27] Yanenko, N.N.: The method of fractional steps; the solution of problems of mathematical physics in several variables, Springer-Verlag, Berlin, 1971
[28] Zhu, M.: Mechanisms for Biological Pattern Formation – Nonlinear Effects, PhD thesis, University of Washington, Seattle, 1994